

Neuronal Projections from V1 to V2 in Amblyopia

Lawrence C. Sincich,¹ Cristina M. Jocson,² and Jonathan C. Horton²

¹Department of Vision Sciences, University of Alabama at Birmingham, Birmingham, Alabama 35294, and ²Beckman Vision Center, University of California, San Francisco, San Francisco, California 94143

The mechanism of amblyopia in children with congenital cataract is not understood fully, but studies in macaques have shown that geniculate synapses are lost in striate cortex (V1). To search for other projection abnormalities in amblyopia, the pathway from V1 to V2 was examined using a triple-label technique in three animals raised with monocular suture. [³H]proline was injected into one eye to label the ocular dominance columns. Cholera toxin B subunit conjugated to gold (CTB-Au) was injected into V2 to label V1 projection neurons. Alternate sections were processed for cytochrome oxidase (CO) and CTB-Au, or dipped for autoradiography. Eight fields of CTB-Au-labeled cells in V1 opposite injection sites were plotted in layers 2/3 or 4B. After thin stripe injection, labeled cells were concentrated in CO patches. Despite column shrinkage, cells in deprived and normal columns were equal in size and density in both layers 2/3 and 4B. After pale or thick stripe injection, labeled cells were concentrated in interpatches. Only 23% of projection neurons originated from deprived columns. This reduction exceeded the degree of column shrinkage, a result explained by the fact that column shrinkage causes disproportionate loss of interpatch territory. These data indicate that early monocular form deprivation does not alter the segregation of patch and interpatch pathways to V2 stripes or cause selective loss or atrophy of V1 projection neurons. The effect of shrinkage of geniculocortical afferents in layer 4C following visual deprivation is not amplified further by attenuation of the amblyopic eye's projections from V1 to V2.

Introduction

In children the most severe form of amblyopia occurs when an eye is deprived of visual stimulation by a dense opacity of the ocular media, such as a congenital cataract. Hubel and Wiesel modeled this form of amblyopia by raising animals with unilateral eyelid suture. In striate cortex, few neurons could be stimulated effectively through the amblyopic eye (Wiesel and Hubel, 1963b; Hubel and Wiesel, 1970). The anatomical correlate of this shift in ocular preference was revealed by the intraocular injection of a transneuronal tracer, [³H]proline. The deprived eye's ocular dominance columns in layer 4C were reduced in surface area, whereas those belonging to the normal eye were expanded (Hubel et al., 1977; Shatz and Stryker, 1978; LeVay et al., 1980; Swindale et al., 1981). In contrast, monocular suture in adult animals produced no column shrinkage. Hubel and Wiesel (1970) proposed that visual deprivation during a critical period early in life causes loss of geniculate synapses onto cortical cells serving the impaired eye. This anatomical change was thought to be responsible for amblyopia, by reducing the flow of visual signals from the deprived eye to striate cortex (Wiesel, 1982).

This explanation is appealing, but does not account fully for the severe amblyopia that ensues after early monocular form de-

privation. Eyelid suture, beginning at 2 weeks of age, reduces visual acuity to the level of sensing only hand motions (Sparks et al., 1986). However, the deprived eye's ocular dominance columns still occupy ~30% of layer 4C (Horton and Hocking, 1997). The fact that layer 4C continues to receive a sizable input from the deprived eye implies that additional anatomical changes at subsequent levels of visual processing may also contribute to amblyopia. In macaques with amblyopia from strabismus and anisometropia, Kiorpes et al. (1998) observed that neurons in V1 show altered receptive field properties, but the abnormalities were too mild to explain the depth of amblyopia. They proposed that serial deficits in cortical function occur in amblyopia, affecting both striate cortex and extrastriate cortex.

V1 sends most of its output to V2, making this neuronal projection a logical starting point for testing the effects of amblyopia on extrastriate cortex. V1 cells located in ocular dominance columns serving opposite eyes project onto binocular cells in V2. This convergence of ocular signals should maximize the potential for direct competition between the eyes, therefore rendering this projection particularly vulnerable to monocular deprivation. In contrast, the competition in V1 between geniculocortical afferents is confined mainly to the borders of ocular dominance columns in layer 4C, because these are the principal regions where axon terminals have access to binocular cells (LeVay et al., 1980).

To investigate the impact of amblyopia on the V1 to V2 pathway, tracer injections were made into V2 in macaques raised with monocular eyelid suture. The density of retrogradely labeled cells in V1 was compared in ocular dominance columns serving the deprived eye and the normal eye. The main goal was to determine whether a selective loss of projections from V1 patches or interpatches serving the deprived eye contributes to reduction of visual function in amblyopia (Fig. 1).

Received Sept. 20, 2011; revised Dec. 7, 2011; accepted Jan. 4, 2012.

Author contributions: L.C.S. and J.C.H. designed research; L.C.S. and J.C.H. performed research; L.C.S., C.M.J., and J.C.H. analyzed data; L.C.S. and J.C.H. wrote the paper.

This work was supported by Grants EY10217 (J.C.H.), EY13676 (L.C.S.), and EY02162 (Beckman Vision Center) from the National Eye Institute, and by the Disney Award from Research to Prevent Blindness. The California Regional Primate Research Center is supported by NIH Base Grant RR00169. We thank Valerie L. Wu for technical assistance.

Correspondence should be addressed to Dr. Jonathan C. Horton, Beckman Vision Center, University of California, San Francisco, 10 Koret Way, San Francisco, CA 94143-0730. E-mail: hortonj@vision.ucsf.edu.

DOI:10.1523/JNEUROSCI.4799-11.2012

Copyright © 2012 the authors 0270-6474/12/322648-09\$15.00/0

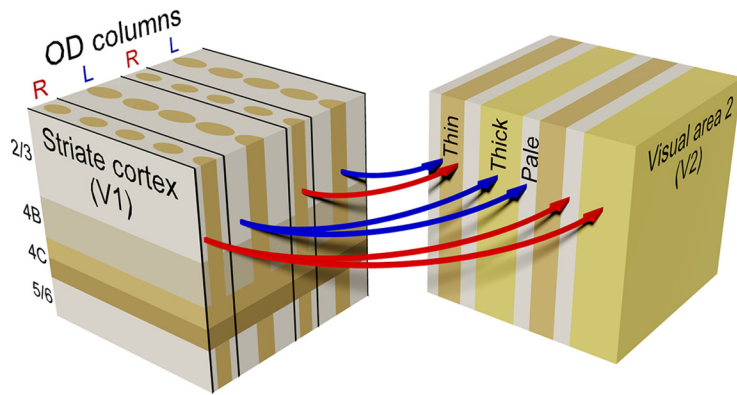


Figure 1. Projections from V1 to V2 in amblyopia. Visual deprivation of the right eye causes shrinkage of ocular dominance (OD) columns and reduction in the size of CO patches. Although the CO patches are smaller, they occupy a greater percentage of the deprived eye's columns. The appearance of the thin, pale, and thick stripes in V2 remains normal in amblyopia. In this study, the layer 3 projections were compared from normal eye columns (blue arrows) and deprived eye columns (red arrows) to V2 stripes, as well as those from layer 4B (not illustrated).

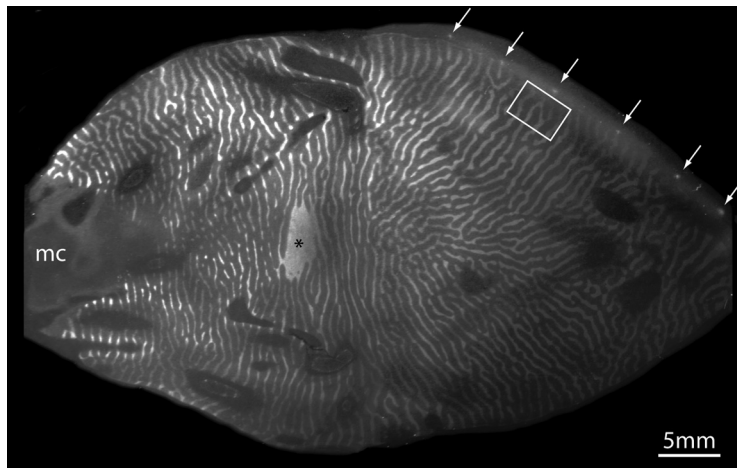


Figure 2. Shrinkage of ocular dominance columns. Autoradiograph of a single tangential section cut through a flatmount of the right striate cortex from a monkey that underwent right eye suture at age 20 d. [^3H]proline was injected into the right eye when the animal was adult to label the ocular dominance columns in layer 4C. They appear bright in this darkfield image, and are shrunken relative to the unlabeled ocular dominance columns serving the normal left eye. The CTB-Au injections (arrows) in V2 are visible near the dorsal V1 border of the operculum, because the D-19 developer produced some silver enhancement. Rectangle is shown at higher magnification in Figure 5a. mc, Monocular crescent. The asterisk represents the left eye's blind spot.

Materials and Methods

Experimental procedures. Three rhesus monkeys (*Macaca mulatta*) born at the California National Primate Research Center (CNPRC) were used for these experiments. The animals underwent unilateral eyelid suture at ages 8 (male), 19 (female), and 20 (male) d. Tarsorrhaphy was performed under general anesthesia with ketamine HCl (10 mg/kg, i.m.) supplemented with local anesthesia consisting of 2% lidocaine with epinephrine 1:100,000. The lid margins of the right eye were trimmed with scissors and closed with interrupted 6-0 Vicryl horizontal mattress sutures. The animals were raised at the CNPRC and transferred after age 5 years to University of California (UC) San Francisco for anatomical labeling of the projection from V1 to V2.

The projection from V1 to V2 was labeled as described previously (Sincich and Horton, 2002, 2005; Sincich et al., 2007). After the animal was anesthetized with 2% isoflurane, 5–6 pressure injections of 140 nl of a retrograde tracer, 0.1% cholera toxin B subunit conjugated to gold (CTB-Au; List Biological) (Llewellyn-Smith et al., 1990), were made into exposed V2 located along the posterior edge of the lunule sulcus. The cytochrome oxidase (CO) stripes in V2 are not visible *in vivo*, so the injections were made blindly, expecting that some would land in the middle of a stripe. The injections were spaced ~5 mm apart in each

hemisphere to produce nonoverlapping fields of retrogradely labeled cells in V1. Injection depth was ~1 mm, centered in layers 3 and 4, which receive the densest input from V1 (Rockland and Virga, 1990).

After the tracer injections were finished, the tarsorrhaphy was opened and 2 mCi of L-[2,3,4,5- ^3H]proline (PerkinElmer) were injected into the vitreous of the right eye to label the ocular dominance columns by transneuronal autoradiography. Each animal received buprenorphine (0.02 mg/kg, i.m.), an opiate analgesic, until it had recovered from the surgical procedures. Experimental protocols were approved by the appropriate Institutional Animal Care and Use Committees at UC Davis and UC San Francisco.

After a week to allow time for tracer transport, the monkey was killed with pentobarbital (150 mg/kg) and perfused with normal saline followed by 1 L of 1% paraformaldehyde in 0.1 M phosphate buffer, pH 7.4. Cortex containing V1 and V2 from each occipital lobe was flat-mounted (Horton and Hocking, 1996a). The first 10 sections were cut tangentially at 40 μm with a freezing microtome and processed for CO (Wong-Riley, 1979). Thereafter, alternating sections were cut either for autoradiography (30 μm) or CO (40 μm). The CO sections were coverslipped temporarily with 0.1 M phosphate buffer to photograph the injection sites and the pattern of CO staining in V1 and V2 before silver enhancement of CTB-Au. The pipette left a small, purple deposit at each V2 injection site that could be located by searching near the V1 border. After the injections were identified and categorized by stripe type, the CO sections were silver-intensified with an IntenSE-M kit (GE Healthcare) to visualize the CTB-Au-labeled cells. Autoradiographs were processed as described previously (Horton and Hocking, 1997). Borders of the ocular dominance columns were defined by thresholding autoradiographs to allocate 30% of layer 4C β to the deprived eye. This value corresponded closely to judgments made by eye regarding column borders. The data were also analyzed using values between 20 and 40%. Over this

range, comparisons between normal and deprived columns of projection cell density yielded consistent conclusions, indicating that the exact area assigned to deprived columns was not a critical parameter. Sections were aligned using radial blood vessels to compare autoradiographs with CO sections.

Data analysis. There were 38 injections in the three monkeys. Eight representative injections that were well centered in clearly identifiable stripes (4 thin, 2 pale, 2 thick) were studied quantitatively. The single, most densely labeled section in layer 2/3 was selected for analysis. The position of every CTB-Au-labeled cell, viewed in a microscope in darkfield illumination through crossed polarizing filters at 200 \times magnification, was plotted on a Wacom Cintiq display tablet located underneath a camera lucida using AutoCAD 2002 (Autodesk). Cells were also plotted in a single section through layer 4B.

The same layer 2/3 section used to plot cells was used to define the CO patches in V1. A grayscale digital photograph was taken with polarizing filters, semicrossed to scatter the light so that the opacity of the silver in transmitted light was neutralized. This procedure insured that the silver in the labeled cells did not confound assessment of CO density in the section. Holes from major blood vessels were filled in with pixels of the mean image grayscale value using Photoshop CS (Adobe Systems). A

low-pass Fourier-filtered image was subtracted from the original image using Matlab (Mathworks) to eliminate unevenness in CO staining across the flatmount section. Next, the image was blurred with a Gaussian filter ($\sigma = 45 \mu\text{m}$) and divided into six zones of equal area based on the CO density. The darkest two zones were defined as patches (Purves and LaMantia, 1993; Farias et al., 1997).

A two-way χ^2 test was used to determine whether the density of labeled cells in patches versus interpatches differed significantly from a random distribution. It was also used to determine whether the density of cells in deprived columns versus normal columns differed from a random distribution, for both patch and interpatch compartments.

After thin stripe injection, labeled cells were located in clusters in V1. To calculate their local density, regions of cortex devoid of labeled cells were excluded. This operation was performed in Matlab by carrying out a Delaunay triangulation on the plot of cells to identify the shortest leg for each triangle formed by three cells. The median length of the shortest legs was defined as the median distance between each CTB-Au-labeled cell and its nearest neighbor. Next, the scatterplot of cell locations was convolved with a two-dimensional Gaussian filter, whose half-width at half-height equaled this

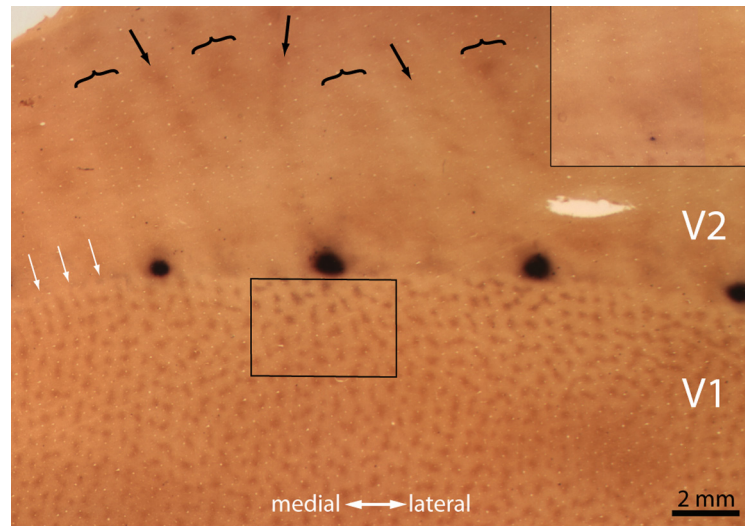


Figure 3. CTB-Au tracer injection into a thin stripe. Layer 3 CO section after silver enhancement, showing four CTB-Au injections in V2, close to the V1 border. The rectangle indicates the field of retrogradely labeled V1 cells analyzed in Figures 4 and 5. The inset at upper right shows the CTB-Au injection site for this field before silver enhancement. The injection is small and well centered in a thin stripe. The white arrows denote rows of small, pale CO patches, aligned with the deprived eye's ocular dominance columns in layer 4C. Black arrows show thin stripes, brackets show thick stripes.

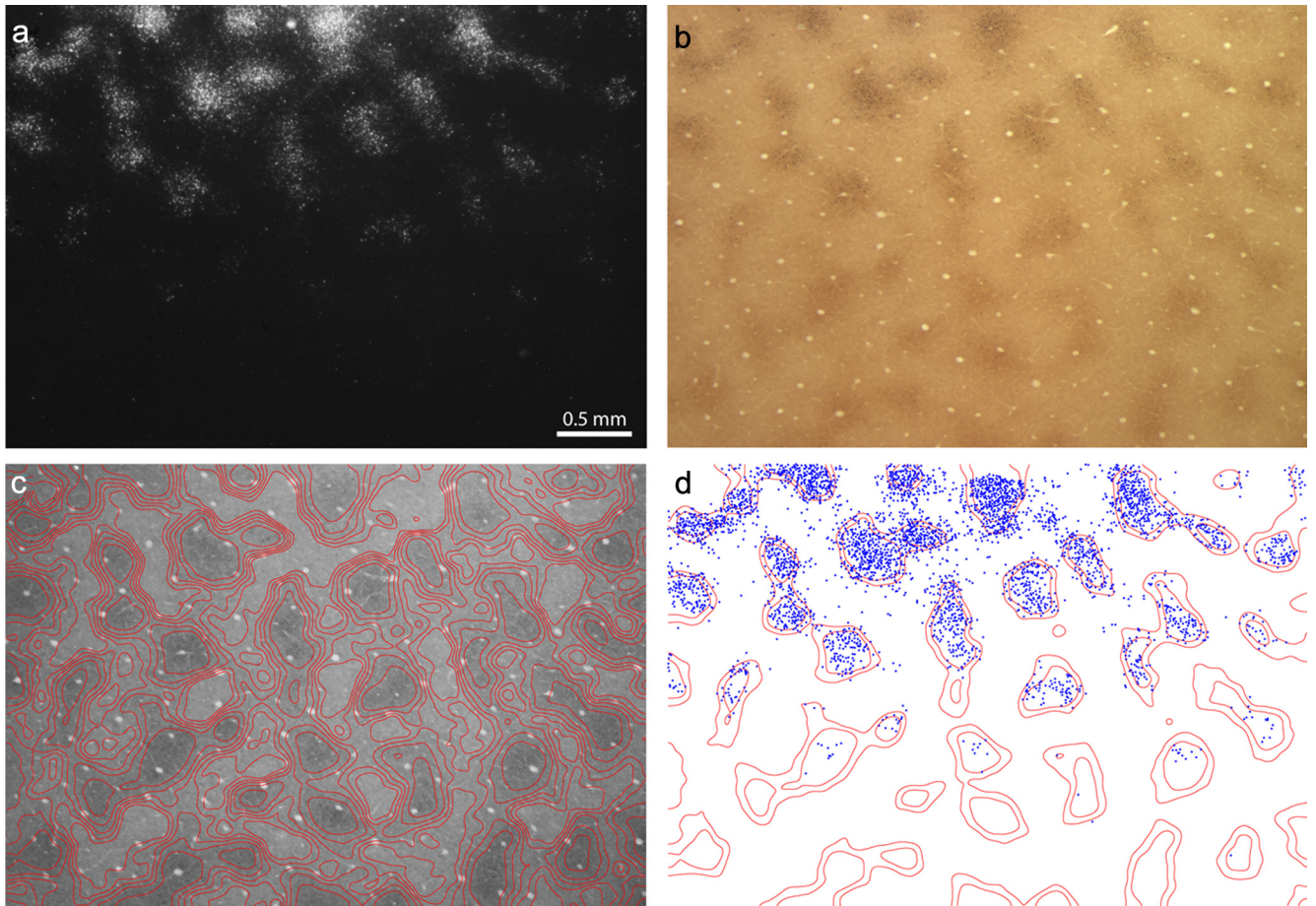


Figure 4. Thin stripe CTB-Au injection labels cells in patches. *a*, Darkfield image showing clusters of retrogradely filled cells. The field is enclosed by the rectangle in Figure 3. *b*, Identical section in brightfield, showing the CO patches in layer 3, coinciding with the clusters of labeled cells in *a*. *c*, Density contours, superimposed on *b*, to divide CO activity into six zones of equal area. *d*, Plot of CTB-Au-filled cells in *a*, showing their relationship to the CO patches, which correspond to the darkest two zones (33%) in *c*.

median nearest neighbor distance. The convolution resulted in a grayscale image of the cell scatterplot. The grayscale image was then thresholded to include 95% of all pixels above zero to define the area used for cell density calculations. This operation was not useful after pale or thick stripe injection, because the labeled cells in V1 were widely dispersed compared with their distribution after thin stripe injection.

For cell size measurements, individual CTB-Au-labeled neurons were viewed at 1000 \times with an oil-immersion lens in the light microscope and their outlines were traced on a display tablet using the camera lucida. Cell areas were calculated from the outlines using Matlab. To determine the number of cells to measure in normal eye columns or deprived eye columns, a power analysis was performed. With $\alpha = 0.05$, a sample size of 285 cells for each test group was necessary to detect a 7.5% difference in soma area with a power of 0.80. In the lateral geniculate body, monocular suture produces a 24% shrinkage of cell bodies (Hubel et al., 1977). In layer 4C β , monocular enucleation causes a 10% shrinkage of cell bodies (Horton and Hedley-Whyte, 1984), but monocular suture has no effect (Hubel et al., 1977). In this context, a 7.5% difference in cell body size seemed like a reasonable threshold for detecting an effect of amblyopia on V1 projection neurons.

A sample of cells was selected randomly for area measurements, with a probability of selection equal to desired sample size/total cell number in normal eye columns or desired sample size/total cell number in deprived eye columns. Identifying cells in the field plots for inclusion before actual area measurement avoided selection bias due to strength of CTB-Au labeling.

Results

In V1, cytochrome oxidase histochemistry reveals a regular array of dark patches, also known as blobs or puffs. The patches are arranged in rows, each running down the middle of an ocular dominance column (Horton, 1984). In V2, CO labels a repeating pattern of pale–thin–pale–thick stripes (Tootell et al., 1983; Horton, 1984). Neurons in patches project to thin stripes, whereas those in interpatch regions project to pale stripes and thick stripes (Sincich and Horton, 2002). We examined the effect of visual deprivation on these two separate projections (Fig. 1).

Projections to thin stripes in amblyopia

Figure 2 shows an autoradiograph from a monkey whose right eyelids were sutured 3 weeks after birth to generate amblyopia. When the animal was a mature adult, an injection of [^3H]proline was made into the right eye to label the ocular dominance columns. They appeared moderately shrunken throughout V1, consistent with prior accounts of the effect of early monocular visual deprivation (LeVay et al., 1980; Swindale et al., 1981; Horton and Hocking, 1997).

Figure 3 shows a section from the same monkey containing a series of CTB-Au tracer injections placed in V2, near the V1 border. The typical pattern of V2 stripes was visible, alternating between zones of pale–thin–pale–thick CO activity. Despite amblyopia, the stripe pattern in V2 appeared indistinguishable from normal. This was apparent in all three deprived animals. In V1, the CO patches in upper layer rows in register with the deprived ocular dominance columns were slightly smaller and paler, as described previously in occlusion amblyopia (Horton and Stryker, 1993; Horton and Hocking, 1997).

Each tracer injection in V2 produced a field of retrogradely labeled neurons directly across the border in V1. Figure 4 shows ~ 20 clusters of CTB-Au-filled cells resulting from a single thin stripe injection. Looking at the section under darkfield and light-field illumination (compare Fig. 4, *a* and *b*), it is apparent that the clusters of labeled cells coincide with the CO patches. The major point, a principal finding of this study, was that every CO patch was richly labeled: there was no indication that the cell labeling

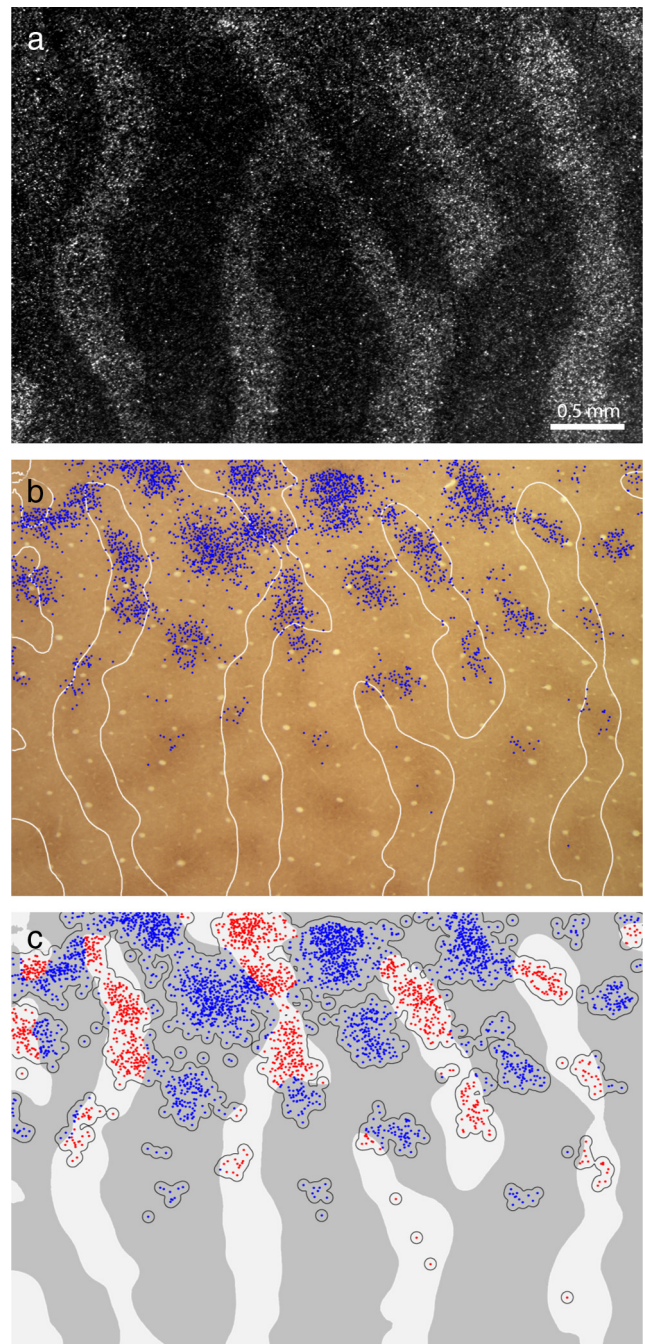


Figure 5. Identification of normal eye and deprived eye patches. *a*, Ocular dominance columns from the box in Figure 2, at higher magnification. *b*, Boundaries of the ocular dominance columns in *a*, with the cells in Figure 4*d* plotted on the CO section in Figure 4*b*. *c*, Cells in *b*, plotted in blue for normal eye columns and in red for deprived eye columns. The boundary surrounding the cells was used to define areas for cell density measurements (see Materials and Methods).

was absent or weaker in every other row, as one might expect if the deprived eye's projection to V2 were lost or attenuated.

The density of CO staining was divided into six zones of equal area, with the darkest two zones representing patches (Fig. 4*c*). The position of each CTB-Au-filled neuron was plotted (Fig. 4*d*). There were 3802 cells, with 2986 (78%) located in patches. If cells were randomly distributed in V1, only 33% would be expected in patches; a χ^2 test confirmed that cells were significantly more likely to be located in patches than interpatches ($p < 0.001$). The

other three thin stripe injections also showed a significant bias, with 61%, 71%, and 93% of cells in patches. In normal animals, 81% (range 64–92%, $n = 8$) of cells were located in patches after thin stripe injection (Sincich and Horton, 2005). Therefore, amblyopia did not disrupt the basic arrangement of the V1 to V2 projection, which is characterized by a segregated pathway from patches to thin stripes.

To quantify the impact of visual deprivation, the distribution of labeled neurons in layer 3 of V1 was compared with the layout of the ocular dominance columns. Figure 5*a* shows the region enclosed by the rectangle in Figure 2. The labeled columns from the amblyopic eye were reduced in width. The autoradiograph was thresholded at 30% to define the columns borders in layer 4C β . In Figure 5*b* they are superimposed on a plot of the labeled cells in the CO section. There were 2482 cells in the normal eye's columns versus 1320 cells in the deprived eye's columns. Only 35% of the cells comprising the projection to V2 were situated in the deprived eye's columns. This reduction was not surprising given the marked shrinkage in surface area of the deprived eye's columns.

The reduction in the V1 to V2 projection from 50% to 35% could simply reflect the shrinkage of ocular dominance columns. Alternatively, the dropout of projections from deprived patches could be disproportionate, exceeding what one would expect merely from column shrinkage. To address this issue, the density of labeled cells in V1 was compared.

For this particular thin stripe injection, there were 282 cells/mm² in the normal eye's columns and 344 cells/mm² in the deprived eye's columns. The higher density in the deprived eye's columns seems counterintuitive. It can be explained, however, by noting that column shrinkage involves surrender of interpatch territory, while tending to spare patches, which are located in the middle of ocular dominance columns. Since most CTB-Au-filled cells were located in patches after thin stripe injection, transfer of interpatch territory to the normal eye increased the density of labeled cells in the deprived columns relative to the normal columns.

To neutralize the impact of this confounding factor, cell density was measured only in regions of cortex that actually contained labeled cells. Figure 5*c* shows these regions, outlined by a process described in Materials and Methods, above. They corresponded approximately, but not exactly, to the CO patches containing labeled cells. Confining measurements to these regions yielded a density of 981 cells/mm² in normal columns and 1038 cells/mm² in deprived columns. The expected density of cells, assuming a random distribution in the labeled cortical field, was 1001 cells/mm². The density of cells was 3.7% higher in the deprived columns, but this difference was not significant ($p > 0.05$, χ^2 test).

Data from all four thin stripe injections are summarized in Table 1. The absolute number of labeled cells in the deprived ocular dominance columns was less than in the normal columns: only 33% of labeled cells were located in deprived columns. However, the mean density of neurons in V2-projecting clusters was only 1.4% lower in deprived columns after excluding cortex devoid of labeled cells from the density calculation. None of the

Table 1. Thin stripe injections

Injection number	Cell count			Cell density*		
	Deprived	Total	Deprived ÷ Total	Deprived (cells/mm ²)	Expected (cells/mm ²)	Difference
1	1320	3802	35%	1038	1001	3.7%
2	1388	4951	28%	812	841	−3.4%
3	914	2897	32%	1208	1209	0.0%
4	680	1800	38%	618	657	−5.9%
Mean			33%			−1.4%

*Density measurement was made after excluding cortex that did not contain labeled cells.

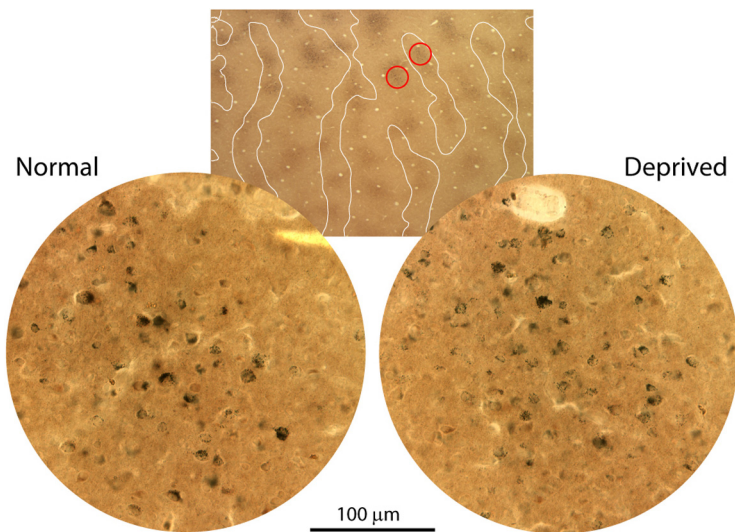


Figure 6. Comparison of layer 3 projection neuron soma size. Examples of two fields, from a normal eye column and a deprived eye column, where cell soma areas were measured by tracing outlines of CTB-Au-filled cells at 1000 \times .

individual injections showed a significant difference in cell density between deprived and normal columns.

Neurons in deprived columns were normal in density after tracer injection into thin stripes. But while their density might be normal, their axon terminal arbors in V2 could be less abundant by analogy with the deprived geniculocortical projection to layer 4C. If so, this change in axon morphology should reduce cell body size. To test this idea, cell soma areas were measured for a sample of labeled cells in normal patches and deprived patches (Fig. 6). The mean soma size was $58.5 \pm 20.9 \mu\text{m}^2$ in normal columns and $59.1 \pm 19.1 \mu\text{m}^2$ in deprived columns (Fig. 7). There was no significant difference in the distribution of soma areas ($p > 0.05$, t test). Measurements in another case, Injection 3, yielded a mean soma size of $55.1 \pm 18.4 \mu\text{m}^2$ ($n = 304$) in normal columns and $55.6 \pm 19.5 \mu\text{m}^2$ ($n = 296$) in deprived columns ($p > 0.05$, t test).

Layer 4B also sends a projection to thin stripes, although it is much less dense than the projection from the upper layers (Sincich et al., 2007). Layer 4B is sandwiched between two layers—4C and 4A—which experience substantial reduction of the geniculocortical projection after eyelid suture. This fact might make layer 4B more vulnerable to the effects of visual deprivation than layer 2/3. Figure 8*a* shows the field of cells in layer 4B that was labeled by the thin stripe injection featured in Figure 3. Just as in layer 2/3, significantly more cells (73%, $p < 0.001$) were situated in patches (Fig. 8*b*). There were 430 cells in the normal eye's columns versus 244 cells in the deprived eye's columns. In labeled regions of cortex (Fig. 8*c*), cell density was 336 cells/mm² in normal eye columns and 347 cells/mm² in deprived eye columns.

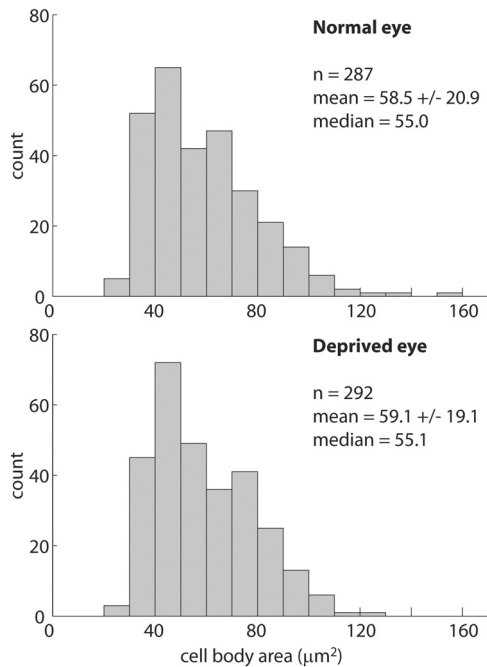


Figure 7. Histograms of soma size. Plot showing cell body areas for projection neurons sampled in patches serving the normal eye and the deprived eye. There was no significant difference between the two populations ($p > 0.05$).

This difference was not significant ($p > 0.05$, χ^2 test). Although fewer layer 4B cells emanated from the deprived eye's columns, their density was normal. Labeled cells were plotted in layer 4B for one other thin stripe injection and their density was equal in deprived columns and normal columns.

Soma cross-sectional areas were measured for retrogradely labeled cells in layer 4B in Figure 8c, following the method outlined above for cells in the upper layers. The mean soma size was $95.0 \pm 41.2 \mu\text{m}^2$ ($n = 351$) in normal columns and $90.3 \pm 42.6 \mu\text{m}^2$ ($n = 215$) in deprived columns. This difference was not significant ($p > 0.05$, t test).

Projections to pale and thick stripes in amblyopia

The distribution of CTB-Au-filled cells in V1 was plotted after two pale stripe injections and two thick stripe injections. As expected, these injections produced denser cell labeling in the interpatches of layer 2/3 (Federer et al., 2009; Sincich et al., 2010). On average, 80% of cells were located in interpatches, whereas only 67% would be expected in this compartment on a random basis ($p < 0.01$, χ^2 test). In normal animals, 84% of cells were present in interpatches after pale or thick stripe injection (Sincich et al., 2010). Thus, visual deprivation did not perturb the segregation of the interpatch to pale/thick stripe projection.

Table 2 shows the number of labeled cells in ocular dominance columns serving the normal eye and the deprived eye after each pale or thick stripe injection. On average, only 23% of V2-projecting cells were located in deprived columns. For every case, the cell density in deprived columns was significantly lower than predicted from a random distribution of cells, with an overall mean reduction of 24%. This reduction was difficult to interpret because the shrinkage of ocular dominance columns occurs by surrender of mostly interpatch territory along column borders. This prime territory contains the highest density of cells that project to pale and thick stripes (Sincich et al., 2010, their Fig. 12). The surviving columns of the deprived eye are comprised of

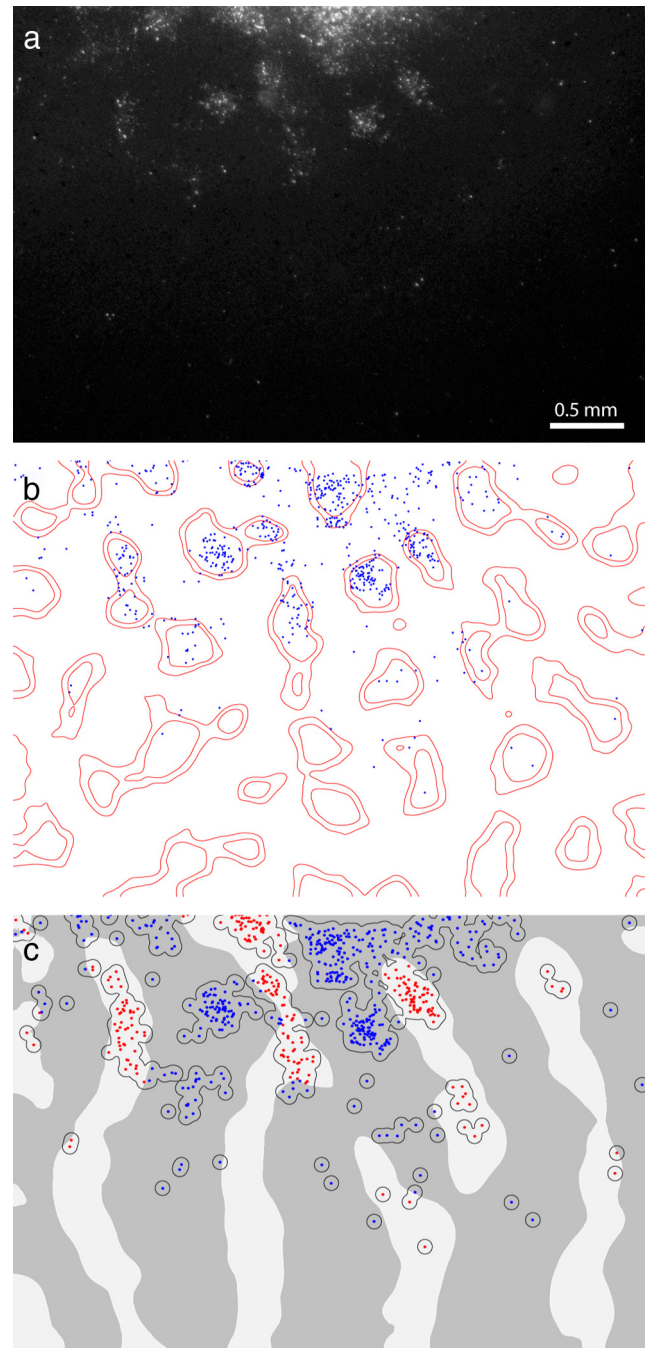


Figure 8. Layer 4B labeling. **a**, Darkfield image of cell labeling in layer 4B from the same region shown in Figures 4 and 5. **b**, Plot of CTB-filled cells, showing their relationship to the patches in layer 3 defined by red contour lines. **c**, Cells in **b**, plotted with respect to the ocular dominance columns (blue, open eye; red, deprived eye).

patches, which contain the lowest density of such cells, and some residual interpatch tissue. Therefore, the low density of projections to pale and thick stripes from deprived columns could merely reflect the loss of prime interpatch cell territory to the other eye, rather than actual dropout of projection neurons serving the deprived eye.

To illustrate this point, we modeled the effect of column shrinkage by distributing 3000 projection neurons in a V1 field of 30 patches in a region of cortex measuring 12 mm^2 (Fig. 9). Eighty-four percent of the cells were placed in interpatches, the average value after a tracer injection into a pale stripe or thick stripe. The patches

were assigned 33% of the cortical area. The effect of visual deprivation was simulated by shrinking the patches in the amblyopic eye's columns to 80% of normal size and by shrinking the ocular dominance columns to a ratio of 30/70. After these operations, patch tissue comprised 43% of the deprived columns and 23% of the normal columns. There were 197 cells/mm² in deprived columns and 270 cells/mm² in normal columns. Given an expected concentration of 250 cells/mm², the density of cells was reduced by 23% in the deprived columns. The close agreement with the reduction of 24% found experimentally suggests that the decrease in density of projection neurons occurred simply because one eye relinquished interpatch territory to the other eye. It is not necessary to postulate that neurons in the deprived eye's columns lost their axonal projections to V2 following eyelid suture.

Discussion

The shrinkage of ocular dominance columns following early visual deprivation provides a striking example of how neuronal connections in the brain can be altered by abnormal sensory experience (Hubel et al., 1977; Wiesel, 1982). Since this landmark discovery, the field has made only modest advances in describing the anatomical changes that occur in amblyopia. It is clear that major physiological deficits are present beyond V1, in extrastriate areas such as V2 and MT (Jones et al., 1984; Imamura et al., 1997; El-Shamayleh et al., 2010; Hess et al., 2010; Bi et al., 2011). It is possible that these abnormalities are due entirely to loss of geniculocortical synapses in layer 4C serving the deprived eye. It seems more likely, however, that synaptic changes at multiple levels, from the lateral geniculate body to higher association areas, combine in series to impair visual function (Kiorpes, 2006).

In monkeys raised with eyelid suture, ~20% of cells outside layer 4C still respond to visual stimulation via the deprived eye. To early investigators, these units seemed to have normal orientation selectivity (Hubel et al., 1977; Blakemore et al., 1978). However, optical imaging in kittens has shown convincingly that orientation tuning is degraded by monocular deprivation (Kim and Bonhoeffer, 1994; Crair et al., 1997). It is unknown how projections from layer 4C to other layers are affected by form deprivation. A precise description of any intracortical wiring abnormalities might explain why orientation selectivity is affected and shed further light on the anatomical changes responsible for amblyopia. Unfortunately, this objective is not attainable with currently available neuroanatomical methods. Probing intracortical connections by extracellular injection of retrograde tracers, even into single layers, is fraught by uptake into dendrites, fibers of passage, and local axon collaterals (Fitzpatrick et al., 1985; Lachica et al., 1992). These problems make it difficult to explore vertical cortical projections, although this approach has been used for horizontal projections in strabismic monkeys to demonstrate selective loss of connections between cells in ocular dominance columns serving opposite eyes (Tychsen et al., 2004). In the future, retrograde viral tracers that cross several synapses may facilitate the examination of wiring abnormalities in amblyopia (DeFalco et al., 2001; Campbell and Herbison, 2007; Callaway,

Table 2. Thick and pale stripe injections

Injection number	Stripe type	Cell count			Cell density		
		Deprived	Total	Deprived ÷ Total	Deprived (cells/mm ²)	Expected (cells/mm ²)	Difference
5	Thick	404	2389	17%	114	199	–43%
6	Thick	1023	3888	26%	302	348	–13%
7	Pale	388	1757	22%	152	206	–26%
8	Pale	737	2913	25%	218	259	–16%
Mean				23%			–24%

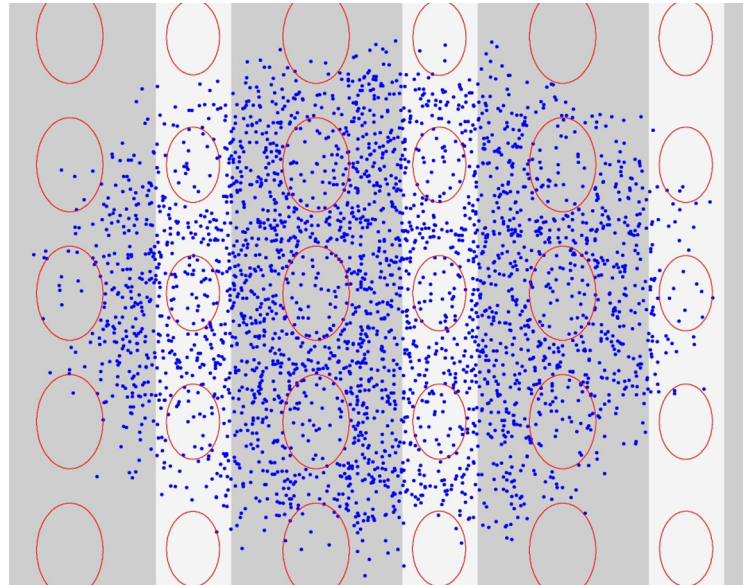


Figure 9. Effect of column shrinkage on projection cell density after tracer injection into a pale or thick stripe. In this simulation, each blue dot represents a cell, with 84% distributed randomly in the interpatches. The oval patches run down the middle of the ocular dominance columns, with the open eye's columns (gray stripes) expanded to fill 70% of the cortex. The density of projection neurons is 23% lower in the deprived columns (white stripes), simply because they have lost interpatch tissue.

2008). A powerful experiment would be to infect a single cell in a layer such as 4B and to compare the number of labeled cells in each set of layer 4C ocular dominance columns, the laminae of the lateral geniculate body, and even the two eyes.

We made retrograde tracer injections in area V2 to test for intercortical wiring anomalies in amblyopia. This approach had the advantage of cleanly labeling projection neurons from V1 to compare their numbers in ocular dominance columns serving either the normal eye or the deprived eye. Tracer injections into V2 always label neurons in both sets of ocular dominance columns (Sincich and Horton, 2005; Sincich et al., 2010). Labeling is never confined to one eye's columns, no matter how small the tracer injection. This observation means that V1 axon terminals preferentially serving the right eye and the left eye are intermingled intimately in V2. This arrangement should maximize the potential for competition between the eyes, resulting in selective loss of V1 connections serving the deprived eye, according to Hebbian principles (Butz et al., 2009).

In fact, we found little evidence for such an effect. The patches corresponding to the deprived eye stained lightly for CO (Fig. 3). This finding indicated that their cells were less active physiologically. Nonetheless, the projection neurons in deprived CO patches did not fail to label after tracer injection into thin stripes. In fact, analysis showed that the clusters of labeled projection neurons had the same density in normal columns and deprived columns (Table 1). In terms of absolute numbers, only 33% of

cells projecting to thin stripes were located in deprived columns. This reduction was commensurate with the amount of lost cortical territory. The effect of column shrinkage was not amplified further by selective dropout of cell projections from deprived patches to V2. One might wonder why shrinkage of ocular dominance columns caused any loss of projection neurons to thin stripes, given that patches are located in the center of ocular dominance columns. The reason is that ~20% of neurons that project to thin stripes are actually located in interpatch zones. In addition, neurons are exchanged along bridges between patches in adjacent ocular dominance columns (Fig. 5C).

After pale or thick stripe injection, only 23% of projection neurons were located in deprived columns and their density was reduced by 24% (Table 2). A model of the impact of visual deprivation showed that these changes could be accounted for by column shrinkage, without postulating selective dropout of projection neurons in deprived columns (Fig. 9).

Of course, connections to V2 might be lost without any reduction in the number of retrogradely labeled cells in V1. The geniculocortical projection provides an instructive precedent: visual deprivation causes shrinkage of axon terminals in layer 4C but no loss of cells in the lateral geniculate body. The only sign of visual deprivation at the level of the geniculate body is a change in cell size (Wiesel and Hubel, 1963a; Guillery and Stelzner, 1970; Headon et al., 1985). This motivated us to measure the size of projection neurons in normal columns and deprived columns. There was no difference in either layer 4B or 2/3. This suggests that the eyes' projection neurons supported axon terminal arbors of equal size in V2. This conclusion was supported by the observation that deprived eye patches were labeled as intensely as normal eye patches (Figs. 4a, 6). If their projection neurons had less extensive axon terminal arbors, one would expect them to imbibe less retrograde tracer at injection sites. Had this occurred, deprived patches would have appeared fainter in comparison with normal patches. Ultimately, the definitive way to approach this problem would be to label the axons of individual cells projecting to V2 and reconstruct their terminal arbors (LeVay and Ferster, 1977; Rockland and Virga, 1990; Friedlander et al., 1991). By comparing a large inventory of axons emanating from normal columns and deprived columns, one could determine whether visual deprivation has any impact on axon terminal morphology or synapse number.

The projection from V1 to V2 is adult-like in macaques by age 1 week, and probably even at birth (Kiorpes et al., 2003). The lack of any obvious impact from eyelid suture, even at age 8 d, suggests that either this projection is impervious to the effects of sensory deprivation or its critical period comes at an earlier age. The latter possibility seems unlikely, because it would push the critical period into fetal life. Perhaps structural changes in the V1 to V2 projection are induced by monocular deprivation, but they are too subtle to detect with our experimental approach. For example, synaptic connections in V2 could be corrupted in strength, location, specificity, and chemistry by visual deprivation, without necessarily reducing the uptake of a retrograde tracer. These possibilities aside, it is clear that dramatic contraction of afferents, as seen in the geniculate projection to layer 4C, does not occur. The shrinkage of geniculate arbors in layer 4C may represent an exceptional response to sensory deprivation, rather than a common phenomenon throughout the nervous system.

As mentioned previously, column shrinkage involves surrender of more interpatch tissue than patch tissue. Therefore, in deprived columns, compared with normal columns, a greater proportion of cells projects to thin stripes than to pale or thick

stripes. It is interesting to speculate what consequences this difference might have for visual function in amblyopia. There is evidence that patches are specialized for the processing of color information (Livingstone and Hubel, 1984; Lu and Roe, 2008). Relative sparing of patches could explain why color perception seems to be impaired less severely than spatial resolution in patients with amblyopia (Mangelschots et al., 1996; Almog and Nemet, 2010). However, there is some doubt that color and form are handled by largely segregated cell populations in V1, implying that color processing may not be limited to patches (Gegenfurtner and Kiper, 2003; Shapley and Hawken, 2011). Moreover, at low spatial frequencies, color and luminance discrimination are similarly affected in most amblyopes (Bradley et al., 1986; Mullen et al., 1996). Finally, it is worth recalling that in most forms of amblyopia, there is no shrinkage of ocular dominance columns (Horton and Stryker, 1993; Horton and Hocking, 1996b). Therefore, in the majority of patients, amblyopia does not have a greater impact on interpatch projections to V2.

We have examined the impact of early form deprivation—which produces the most severe type of amblyopia—on the projections between V1 and V2. To our surprise, the effect predicted from the shrinkage of ocular dominance columns in V1 was not found. There was no evidence for loss or atrophy of V2 projection neurons in deprived ocular dominance columns. Instead, the changes in projection neuron density were commensurate with column shrinkage. This finding is encouraging from a clinical standpoint. If one could devise a treatment that restored a normal geniculocortical projection in layer 4C, the downstream pathways at the disposal of the deprived eye might still be quite functional.

References

- Almog Y, Nemet A (2010) The correlation between visual acuity and color vision as an indicator of the cause of visual loss. *Am J Ophthalmol* 149:1000–1004.
- Bi H, Zhang B, Tao X, Harwerth RS, Smith EL 3rd, Chino YM (2011) Neuronal responses in visual area v2 (v2) of macaque monkeys with strabismic amblyopia. *Cereb Cortex* 21:2033–2045.
- Blakemore C, Garey LJ, Vital-Durand F (1978) The physiological effects of monocular deprivation and their reversal in the monkey's visual cortex. *J Physiol* 283:223–262.
- Bradley A, Dahlman C, Switkes E, De Valois K (1986) A comparison of color and luminance discrimination in amblyopia. *Invest Ophthalmol Vis Sci* 27:1404–1409.
- Butz M, Wörgötter F, van Ooyen A (2009) Activity-dependent structural plasticity. *Brain Res Rev* 60:287–305.
- Callaway EM (2008) Transneuronal circuit tracing with neurotropic viruses. *Curr Opin Neurobiol* 18:617–623.
- Campbell RE, Herbison AE (2007) Definition of brainstem afferents to gonadotropin-releasing hormone neurons in the mouse using conditional viral tract tracing. *Endocrinology* 148:5884–5890.
- Crair MC, Ruthazer ES, Gillespie DC, Stryker MP (1997) Relationship between the ocular dominance and orientation maps in visual cortex of monocularly deprived cats. *Neuron* 19:307–318.
- DeFalco J, Tomishima M, Liu H, Zhao C, Cai X, Marth JD, Enquist L, Friedman JM (2001) Virus-assisted mapping of neural inputs to a feeding center in the hypothalamus. *Science* 291:2608–2613.
- El-Shamayleh Y, Kiorpes L, Kohn A, Movshon JA (2010) Visual motion processing by neurons in area MT of macaque monkeys with experimental amblyopia. *J Neurosci* 30:12198–12209.
- Farias MF, Gattass R, Piñón MC, Ungerleider LG (1997) Tangential distribution of cytochrome oxidase-rich blobs in the primary visual cortex of macaque monkeys. *J Comp Neurol* 386:217–228.
- Federer F, Ichida JM, Jeffs J, Schiessl I, McLoughlin N, Angelucci A (2009) Four projection streams from primate V1 to the cytochrome oxidase stripes of V2. *J Neurosci* 29:15455–15471.
- Fitzpatrick D, Lund JS, Blasdel GG (1985) Intrinsic connections of macaque striate cortex: afferent and efferent connections of lamina 4C. *J Neurosci* 5:3329–3349.

- Friedlander MJ, Martin KA, Wassenhove-McCarthy D (1991) Effects of monocular visual deprivation on geniculocortical innervation of area 18 in cat. *J Neurosci* 11:3268–3288.
- Gegenfurtner KR, Kiper DC (2003) Color vision. *Annu Rev Neurosci* 26:181–206.
- Guillery RW, Stelzner DJ (1970) The differential effects of unilateral lid closure upon the monocular and binocular segments of the dorsal lateral geniculate nucleus in the cat. *J Comp Neurol* 139:413–421.
- Headon MP, Sloper JJ, Hiorns RW, Powell TP (1985) Effects of monocular closure at different ages on deprived and undeprived cells in the primate lateral geniculate nucleus. *Brain Res* 350:57–78.
- Hess RF, Thompson B, Gole GA, Mullen KT (2010) The amblyopic deficit and its relationship to geniculo-cortical processing streams. *J Neurophysiol* 104:475–483.
- Horton JC (1984) Cytochrome oxidase patches: a new cytoarchitectonic feature of monkey visual cortex. *Philos Trans R Soc Lond B Biol Sci* 304:199–253.
- Horton JC, Hedley-Whyte ET (1984) Mapping of cytochrome oxidase patches and ocular dominance columns in human visual cortex. *Philos Trans R Soc Lond B Biol Sci* 304:255–272.
- Horton JC, Hocking DR (1996a) Intrinsic variability of ocular dominance column periodicity in normal macaque monkeys. *J Neurosci* 16:7228–7239.
- Horton JC, Hocking DR (1996b) Pattern of ocular dominance columns in human striate cortex in strabismic amblyopia. *Vis Neurosci* 13:787–795.
- Horton JC, Hocking DR (1997) Timing of the critical period for plasticity of ocular dominance columns in macaque striate cortex. *J Neurosci* 17:3684–3709.
- Horton JC, Stryker MP (1993) Amblyopia induced by anisometropia without shrinkage of ocular dominance columns in human striate cortex. *Proc Natl Acad Sci U S A* 90:5494–5498.
- Hubel DH, Wiesel TN (1970) The period of susceptibility to the physiological effects of unilateral eye closure in kittens. *J Physiol* 206:419–436.
- Hubel DH, Wiesel TN, LeVay S (1977) Plasticity of ocular dominance columns in monkey striate cortex. *Philos Trans R Soc Lond B Biol Sci* 278:377–409.
- Imamura K, Richter H, Fischer H, Lennerstrand G, Franzén O, Rydberg A, Andersson J, Schneider H, Onoe H, Watanabe Y, Långström B (1997) Reduced activity in the extrastriate visual cortex of individuals with strabismic amblyopia. *Neurosci Lett* 225:173–176.
- Jones KR, Spear PD, Tong L (1984) Critical periods for effects of monocular deprivation: differences between striate and extrastriate cortex. *J Neurosci* 4:2543–2552.
- Kim DS, Bonhoeffer T (1994) Reverse occlusion leads to a precise restoration of orientation preference maps in visual cortex. *Nature* [Erratum (1994) 372:196] 370:370–372.
- Kiorpes L (2006) Visual processing in amblyopia: animal studies. *Strabismus* 14:3–10.
- Kiorpes L, Kiper DC, O'Keefe LP, Cavanaugh JR, Movshon JA (1998) Neuronal correlates of amblyopia in the visual cortex of macaque monkeys with experimental strabismus and anisometropia. *J Neurosci* 18:6411–6424.
- Kiorpes L, Doron NN, Movshon JA (2003) Connections of striate cortex in infant macaque monkeys. *Soc Neurosci Abstr* 29:126.7.
- Lachica EA, Beck PD, Casagrande VA (1992) Parallel pathways in macaque monkey striate cortex: anatomically defined columns in layer III. *Proc Natl Acad Sci U S A* 89:3566–3570.
- LeVay S, Ferster D (1977) Relay cell classes in the lateral geniculate nucleus of the cat and the effects of visual deprivation. *J Comp Neurol* 172:563–584.
- LeVay S, Wiesel TN, Hubel DH (1980) The development of ocular dominance columns in normal and visually deprived monkeys. *J Comp Neurol* 191:1–51.
- Livingstone MS, Hubel DH (1984) Anatomy and physiology of a color system in the primate visual cortex. *J Neurosci* 4:309–356.
- Llewellyn-Smith IJ, Minson JB, Wright AP, Hodgson AJ (1990) Cholera toxin B-gold, a retrograde tracer that can be used in light and electron microscopic immunocytochemical studies. *J Comp Neurol* 294:179–191.
- Lu HD, Roe AW (2008) Functional organization of color domains in V1 and V2 of macaque monkey revealed by optical imaging. *Cereb Cortex* 18:516–533.
- Mangelschots E, Beerlandt N, Janssens H, Spileers W (1996) Colour contrast thresholds are normal in functional amblyopia. *Eye (Lond)* 10:479–484.
- Mullen KT, Sankeralli MJ, Hess RF (1996) Color and luminance vision in human amblyopia: shifts in isoluminance, contrast sensitivity losses, and positional deficits. *Vision Res* 36:645–653.
- Purves D, LaMantia A (1993) Development of blobs in the visual cortex of macaques. *J Comp Neurol* 334:169–175.
- Rockland KS, Virga A (1990) Organization of individual cortical axons projecting from area V1 (area 17) to V2 (area 18) in the macaque monkey. *Vis Neurosci* 4:11–28.
- Shapley R, Hawken MJ (2011) Color in the cortex: single- and double-opponent cells. *Vision Res* 51:701–717.
- Shatz CJ, Stryker MP (1978) Ocular dominance in layer IV of the cat's visual cortex and the effects of monocular deprivation. *J Physiol* 281:267–283.
- Sincich LC, Horton JC (2002) Divided by cytochrome oxidase: a map of the projections from V1 to V2 in macaques. *Science* 295:1734–1737.
- Sincich LC, Horton JC (2005) Input to V2 thin stripes arises from V1 cytochrome oxidase patches. *J Neurosci* 25:10087–10093.
- Sincich LC, Jocson CM, Horton JC (2007) Neurons in V1 patch columns project to V2 thin stripes. *Cereb Cortex* 17:935–941.
- Sincich LC, Jocson CM, Horton JC (2010) V1 interpatch projections to V2 thick stripes and pale stripes. *J Neurosci* 30:6963–6974.
- Sparks DL, Mays LE, Gurski MR, Hickey TL (1986) Long- and short-term monocular deprivation in the rhesus monkey: effects on visual fields and optokinetic nystagmus. *J Neurosci* 6:1771–1780.
- Swindale NV, Vital-Durand F, Blakemore C (1981) Recovery from monocular deprivation in the monkey. III. Reversal of anatomical effects in the visual cortex. *Proc R Soc Lond B Biol Sci* 213:435–450.
- Tootell RB, Silverman MS, De Valois RL, Jacobs GH (1983) Functional organization of the second cortical visual area in primates. *Science* 220:737–739.
- Tychsen L, Wong AM, Burkhalter A (2004) Paucity of horizontal connections for binocular vision in V1 of naturally strabismic macaques: cytochrome oxidase compartment specificity. *J Comp Neurol* 474:261–275.
- Wiesel TN (1982) Postnatal development of the visual cortex and the influence of environment. *Nature* 299:583–591.
- Wiesel T, Hubel D (1963a) Effects of visual deprivation on morphology and physiology of cells in the cat's lateral geniculate body. *J Neurophysiol* 26:978–993.
- Wiesel TN, Hubel DH (1963b) Single cell responses in striate cortex of kittens deprived of vision in one eye. *J Neurophysiol* 26:1003–1017.
- Wong-Riley M (1979) Changes in the visual system of monocularly sutured or enucleated cats demonstrable with cytochrome oxidase histochemistry. *Brain Res* 171:11–28.